PHYSICAL REVIEW C

NUCLEAR PHYSICS

THIRD SERIES, VOL. 8, NO. 5 November 1973

Spectroscopy of ^{10}B Levels from the ^{9}Be(d, n)^{10}B Reaction

Yong Sook Park, A. Niiler, and R. A. Lindgren*

U.S. Army Ballistic Research Laboratories, Aberdeen Proving Ground, Maryland 21005

(Received 28 June 1973)

Levels in ^{10}B have been studied with the ^{9}Be(d, n)^{10}B reaction at 7-, 12-, 15-, and 16-MeV incident energy. Neutron angular distributions for transitions to levels below 7 MeV excitation have been measured with a time-of-flight spectrometer, and they have been compared with distorted-wave Born-approximation (DWBA) calculations. Emphasis has been placed on examining the previously reported discrepancy in the $T = 1$ relative spectroscopic factor (S_{rel}) between (d, n) and (^{3}He, d) reactions. It has been found that the discrepancy still exists though to a lesser degree, and that the S_{rel} values from (d, n) appear to be energy-dependent. Sensitivity of calculations to the choices of deuteron-potential sets as well as of other DWBA parameters has been carefully examined in order to extract reliable spectroscopic factors. It has been found that noncutoff DWBA calculations failed to reproduce the detailed structure of the measured angular distributions beyond stripping peaks when "measured" deuteron-potential parameters were used in the calculations. Also excitation functions have been measured at $\theta_{lab} = 15°$ from 14 to 16 MeV in order to check the reaction mechanism for this energy range. The extracted spectroscopic factors compare poorly with the theoretical values of Cohen and Kurath as well as those of Varma and Goldhammer.

I. INTRODUCTION

Siemssen *et al.*[1] reported several years ago that discrepancies existed in relative spectroscopic factors (S_{rel}) between the companion (d, n) and (^{3}He, d) reactions leading to the same final states having different isospin in odd-odd light-mass nuclei. The most distinctive case in which this disparity between (d, n) and (^{3}He, d) was clearly recognized was the ^{10}B nucleus. The S_{rel} value of the $T = 1$ 1.74-MeV level from (d, n) was found to be smaller than that from (^{3}He, d) by as much as a factor of 3 when the spectroscopic factors for the $T = 0$ ground state in both reactions were normalized to 1. This finding was based primarily on the results from the ^{9}Be(d, n)^{10}B reaction studied at 7 MeV by Buccino and Smith[2] and the (^{3}He, d) reaction at 17 MeV by Siemssen *et al.*[1] Since then, both reactions have been studied at lower bombarding energies—the (d, n) at 5.5 MeV and (^{3}He, d) at 10 MeV.[3,4] While there are excellent agreements in S_{rel} values among various (^{3}He, d) reactions,[5] significant differences in S_{rel} values for the $T = 0$ 0.72-MeV level as well as the $T = 1$ 1.74-MeV level are found between the two (d, n) works.

One of the most systematic spectroscopic studies on 1p-shell nuclei via (d, n) reactions was recently made at 11.8 MeV by Mutchler *et al.*[6] The ^{9}Be(d, n)^{10}B reaction, however, was not included in the study. In the case of ^{12}C they found that the agreement between (d, n) and (^{3}He, d) was poor, but there was no consistent discrepancy. In the case of ^{14}N, however, the $T = 1$ S_{rel} discrepancy between the companion reactions was more pronounced. Schiffer *et al.*[7] studied the (d, p) reaction in the 1p shell at 12 MeV. From the ^{9}Be(d, p)-^{10}Be reaction, analog to the ^{9}Be(d, n)^{10}B reaction, no systematic discrepancy in S_{rel} value for $T_>$ states was observed. Couch *et al.*[8] looked for this discrepancy in ^{55}Co via the ^{54}Fe(d, n) reaction at 10 MeV, for which conventional distorted-wave Born-approximation (DWBA) analysis was expected to be more successful than for (d, n) reactions on light-mass nuclei at lower energies. It was concluded that within the limits of experimental and analytical uncertainties there was no discrepancy between (d, n) and (^{3}He, d). Thus it appears that the disparity Siemssen *et al.*[1] have discovered

exists only for odd-odd nuclei or light nuclei.

There has been considerable theoretical interest in this subject during the past several years. Tamura[9] attempted to resolve this discrepancy by incorporating the charge-exchange $\vec{t}\cdot\vec{T}$ term in calculations, but final results pointed in the wrong direction.[10] Cotanch and Robson[11] have indicated that they succeeded in resolving this discrepancy with their new isospin-dependent DWBA formalism, but the final results of their calculations have not been published as yet.

The J^π assignments for levels below 6.0 MeV in ^{10}B have been uniquely established in the literature.[12] There are conflicting reports on J^π for the 6.13- and 6.57-MeV levels. The ^{11}B(^{3}He, α)^{10}B(α_0)-^{6}Li correlation work[13] and ^{6}Li-α scattering[14] assign negative parity for these levels. The previous (d, n) works[2,3] and (^{3}He, d) works[4,5,15] all agree on positive-parity assignment (an $l=1$ transfer) for the 6.56-MeV level, but are still in conflict on the parity assignment for the 6.13-MeV level.

The structure of the positive-parity levels in ^{10}B has been described in detail by Cohen and Kurath[16] with the use of shell-model wave functions constructed on the basis of the 1p shell. More recently, the spectroscopic factors for the 1p-shell nuclei have been calculated also by Varma and Goldhammer[17] using wave functions derived by Goldhammer, Hill, and Nachamkin.[18]

For the reasons mentioned above there seemed to be a need for studying the ^{9}Be$(d, n)^{10}$B reaction at bombarding energies higher than 7 MeV. Thus the ^{9}Be$(d, n)^{10}$B angular distributions were measured for transitions to levels in ^{10}B below 7 MeV excitation at 7, 12, 15, and 16 MeV.[19] Emphasis was focused on the systematic search for the reported discrepancy between (d, n) and (^{3}He, d) as a function of the incident energy. Also, validity of the conventional DWBA analysis of the ^{9}Be(d, n) reaction as well as the sensitivity of the calculations due to distorting parameters have been carefully investigated before extracting spectroscopic information from the data.

II. EXPERIMENTAL PROCEDURE AND RESULTS

A. Experimental Setup

The experiment was carried out at the U. S. Army Ballistic Research Laboratories (BRL) FN tandem Van de Graaff facility. The experimental arrangement in the low-background neutron room of that facility is shown in Fig. 1. A 50- to 70-μA dc beam from a direct-extracting-diode ion source was chopped into 30–40-nsec bursts by a 2-MHz rf voltage applied to a pair of deflecting plates. Bunching to approximately 1.2-nsec pulse width was accomplished by a 4-MHz klystron buncher with a compression ratio of 40:1. Typically an average beam intensity between 0.5 and 1.0 μA was focused onto the target. The target chamber consisted of a stainless-steel cylinder, 10 cm in diameter, 30 cm in height, and with a 1-mm wall thickness. A target holder was positioned at the center of the chamber and could hold up to four targets. After the beam passed through the target, it was stopped in lead about 4.5 m downstream. It was constrained from hitting the inside of the beam tube by two slits, one upstream and one downstream of the target, and was tuned such that less than 1% of the beam was intersected by these slits. The Faraday cup used to measure the beam intensity consisted of the last 3-m section of the beam tube before the Pb beam stop. All cross-section measurements were monitored by both the beam-current integration and a 2-mm-thick silicon-surface-barrier detector, placed at 135° in the target chamber, which detected charged particles from the d+^{9}Be reactions. The targets used were self-supporting foils of ^{9}Be with thicknesses of 2.75 and 0.13 mg/cm^2. Resolution requirements determined which target would be bombarded in any given situation. The target thicknesses were determined by three different methods. The three values, obtained from elastic α scattering at 4.5 MeV, comparison between our elastic deuteron scattering measurement at 15 MeV and the data of Armstrong *et al.*,[20] and a direct weighing of the foil, all agreed to within 15%.

The neutron detector consisted of a NE-213 liquid scintillator, 2.5 cm in thickness and 17.8 cm in diameter, held in a light-tight aluminum can and Lucite-coupled to a XP1041 photomultiplier (PM) tube. This detector could be positioned at a 10-m flight path from the target at every 5° from 0 to 90° and at every 10° from 90 to 160°. It could also be placed at 18.5 m at 7.5 and 90° for very-high-resolution work. The beam line and detector were

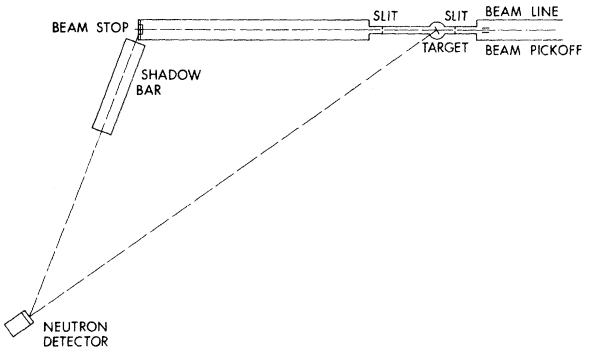

FIG. 1. A schematic diagram of the experimental set-up for (d, n) studies in the neutron room (not drawn to scale).

located at the 5.5-m level of the large 25-m × 25-m × 18-m low-mass room. Thus the experiment could be done in open geometry with the only shielding necessary accomplished by a shadow bar consisting of Pb, Cu, and borated paraffin inserted between the detector and the Pb beam stop.

Neutron energies were determined by time-of-flight (TOF) measurements. A time-to-amplitude converter (TAC) was started by a fast signal derived from the anode of the PM tube and was stopped by a signal obtained from the beam-pickoff tube located just upstream of the target chamber. The over-all timing resolution of this system was about 1.4 nsec full width at half maximum (FWHM). The TAC signal required gating by a twofold coincidence between the neutron-window output of an n-γ discrimination circuit and a signal indicating that the energy-bias level was exceeded by the PM dynode output.

In order to determine absolute cross sections it is necessary to know absolute neutron-detector efficiencies. As calculations of neutron-detector efficiencies above roughly 12 MeV have not shown very good agreement with measured values because of uncertainties on how to handle the ^{12}C$(n, n' 3\alpha)$ reaction in the calculations, it was decided to measure the detector efficiency directly. The experimental conditions required the knowledge of the efficiencies from 10 to 20 MeV for three different bias levels. The three different bias levels were necessary because low-energy backgrounds in the room increased fairly strongly with increasing deuteron-beam energy. The Compton edge from the 662-keV γ ray from ^{137}Cs was used to obtain the reference for the detector bias level. The method of obtaining the absolute detector efficiencies was to measure simultaneously yields from the ^{2}H$(d, n)^{3}$He and ^{2}H$(d, p)^{3}$H reactions with the neutron detector at a given lab angle and the surface-barrier-monitor detector at 135°. A deuterated polyethylene foil was used for the target. The efficiency is then given by

$$\epsilon(E_n) = \frac{Y_{d,n}(E_n)}{Y_{d,p}} \frac{\sigma_{d,p}(\theta_p)}{\sigma_{d,n}(\theta, E_n)} \frac{\Omega_p}{\Omega_n} , \quad (1)$$

where $Y_{d,n}(E_n)$ and $Y_{d,p}$ are the ^{2}H$(d, n)^{3}$He and ^{2}H$(d, p)^{3}$H yields, respectively, $\sigma_{d,n}(\theta_n, E_n)$ and $\sigma_{d,p}(\theta_p)$ are the respective cross sections, and Ω_n and Ω_p are the neutron-detector and monitor-detector solid angles. The ^{2}H(d, n) and ^{2}H(d, p) cross sections were taken from Brolley, Putnam, and Rosen,[21] using the smooth set of Legendre coefficients given therein for our $E_d = 7$ and 12 MeV measurements and extrapolating those curves for the 15-MeV measurements. The accuracy of the cross sections thus determined was taken to be ±5% although the authors quote considerably smaller values. Thus the uncertainty of the efficiency measurement is dominated by the cross-section uncertainties, since the yields and solid angles are known to better than 2%. The total uncertainty on the efficiency was then 8%.

B. Experimental Results

In order to illustrate the resolution capability of the system a TOF spectrum of neutrons from the ^{9}Be$(d, n)^{10}$B reaction was measured at $E_d = 16$ MeV with the detector placed at the 7.5° and 15-m position. Figure 2 shows this spectrum. As can be seen, 1% energy resolution is achieved for 20-MeV neutrons with quite low backgrounds under all peaks of interest, which are labeled by excitation

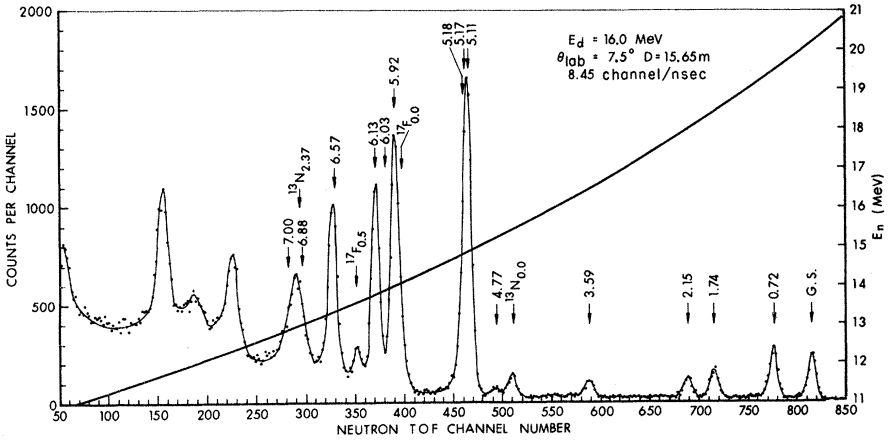

FIG. 2. A neutron time-of-flight spectrum of the ^{9}Be$(d,n)^{10}$B reaction. The spectrum was taken with the thin (0.13-mg/cm^2) self-supporting target The over-all energy resolution was about 1% for 20-MeV neutrons. The width of the pulsed deuteron beam was about 1.25 nsec. The peaks are labeled by excitation energies adopted in Ref. 12.

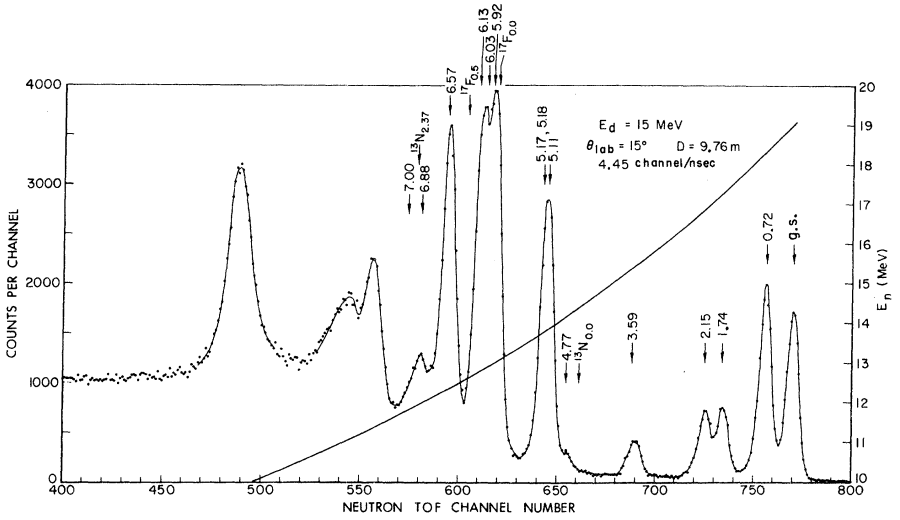

FIG. 3. A neutron time-of-flight spectrum of the ^{9}Be$(d,n)^{10}$B reaction, measured with the thick (2.75-mg/cm^2) self-supporting target. Most of the angular distributions were measured with this target and a shorter (~10-m) flight path in order to accelerate the data accumulation.

energies assigned in Ref. 12. Analysis of the data was not feasible beyond the 6.57-MeV level because of interference from the carbon and oxygen contamination. The population of a 6.03-MeV level of ^{10}B in the present reaction is not confirmed. Even with a higher resolution achieved by going to 7 MeV, no evidence for populating this level could be found.

Most of the angular distributions were measured with the thick target and 10-m flight path, which gave sufficient resolution for separating peaks of interest, in order to accelerate the data-accumulation rate. A typical TOF spectrum measured at 15 MeV and 15° under such a condition is shown in Fig. 3. In order to improve the accuracy in the data analysis an automatic fitting code AUTOFIT [22] was used throughout for peak integration. This enabled us to obtain separate angular distributions for the 5.92- and 6.13-MeV transitions.

Measured angular distributions for transitions to levels in ^{10}B are shown in Figs. 4–7, where they are compared with the corresponding DWBA calculations. The detailed descriptions of the calculations are presented in a later section. The angular distributions measured at 7 MeV are shown here up to 2.15 MeV excitation since this low-energy measurement was only for the purpose of comparing it to the previous (d,n) results at this energy.[2] The 15-MeV angular-distribution measurements were extended to backward angles as shown in Fig. 6, so that the expected j dependence associated with $l=1$ angular distributions could be studied. Combined angular distributions were obtained for the unresolved triplet at 5.1 MeV, and they are compared with the mixture of $l=0$ and $l=1$ calculations with a fixed admixture strength in all cases.

C. Excitation Function and Reaction Mechanism

The analysis of measured angular distributions in terms of conventional DWBA calculations requires, of course, that the reaction goes by a direct one-step process. The question of the reaction mechanism is thus very important especially when spectroscopic factors are to be extracted

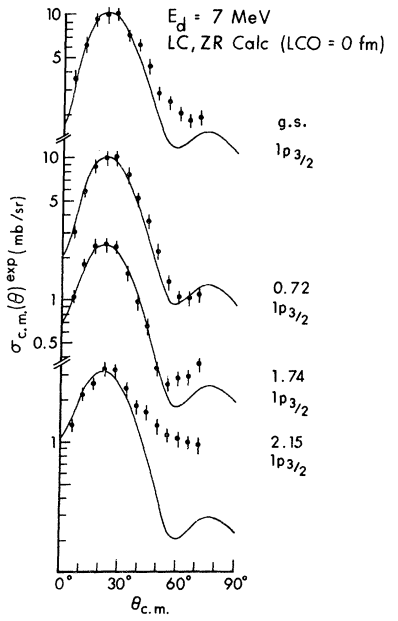

FIG. 4. Angular distributions for transitions to the first four low-lying states in ^{10}B from the ^{9}Be(d,n) reaction at 7 MeV. Solid lines represent noncutoff local zero-range DWBA calculations. Details of the calculations are described in the text.

from the experimental data. Because of the light-mass ^{9}Be$+d$ system, the *a priori* assumption of the dominance of direct process over compound-nucleus process for the ^{9}Be$(d,n)^{10}$B reaction in this energy range should receive a stringent empirical test.

The 15-MeV incident-deuteron energy populates levels at 30 MeV excitation in the ^{11}B compound nucleus, and thus the continuum model of the statistical theory should safely apply. Behavior of the excitation functions for transitions to isolated states in the final nucleus is known to give a clue to the reaction mechanism.

Figure 8 shows the excitation functions for the ^{9}Be$(d,n)^{10}$B reaction measured from 14 to 16 MeV at $\theta_{lab}=15°$, the angle at which the stripping peaks for $l=1$ transitions occur. The solid dots repre-

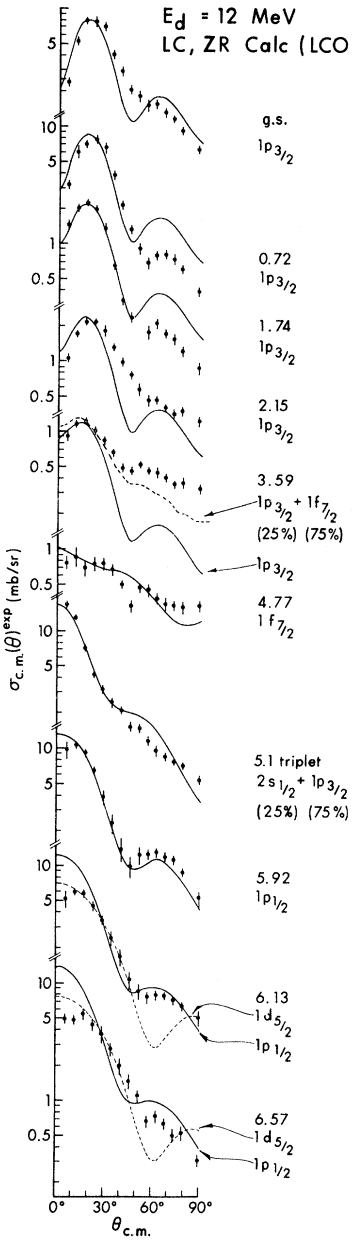

FIG. 5. Angular distributions for transitions to levels below 7 MeV excitation in ^{10}B from the ^{9}Be(d,n) reaction at 12 MeV. The curves represent noncutoff local zero-range DWBA calculations, which were normalized to data arbitrarily. Details of the calculations are described in the text.

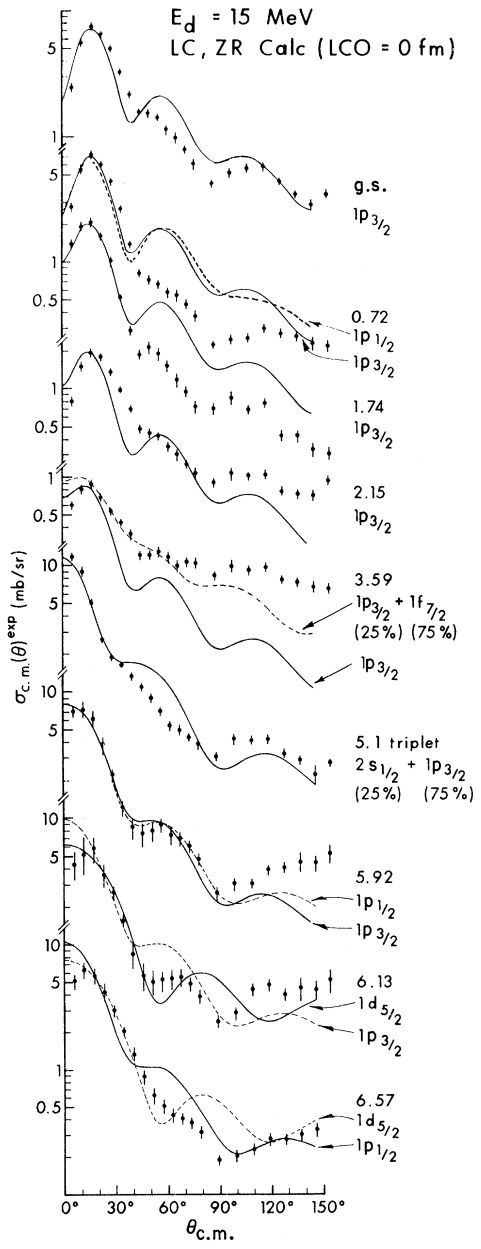

FIG. 6. Angular distributions for 15 MeV. See the caption for Fig. 5 for detail.

sent cross sections measured with the thick target (equivalent to 130-keV beam spread) and 200-keV steps, and the open circles represent cross sections taken with the thin target (equivalent to 8-keV beam spread) and 50-keV steps. The solid lines represent DWBA calculations normalized arbitrarily to the data.

It is clear that strong fluctuations in cross sections as a function of the incident energy, known as a signature of the compound process, are completely missing from these excitation functions. This absence of the rapid and strong random fluctuations in excitation functions together with the strong forward-peaking and well structured oscillatory pattern in the angular distributions shown in Figs. 4–7 support our assumption that the dominant reaction mechanism for the ^{9}Be$(d, n)^{10}$B reaction at these energies is direct and thus largely justifies the present DWBA analysis of the data. The question as to whether the reaction is dominated by a one-step or two-step process cannot be answered from this analysis, of course.

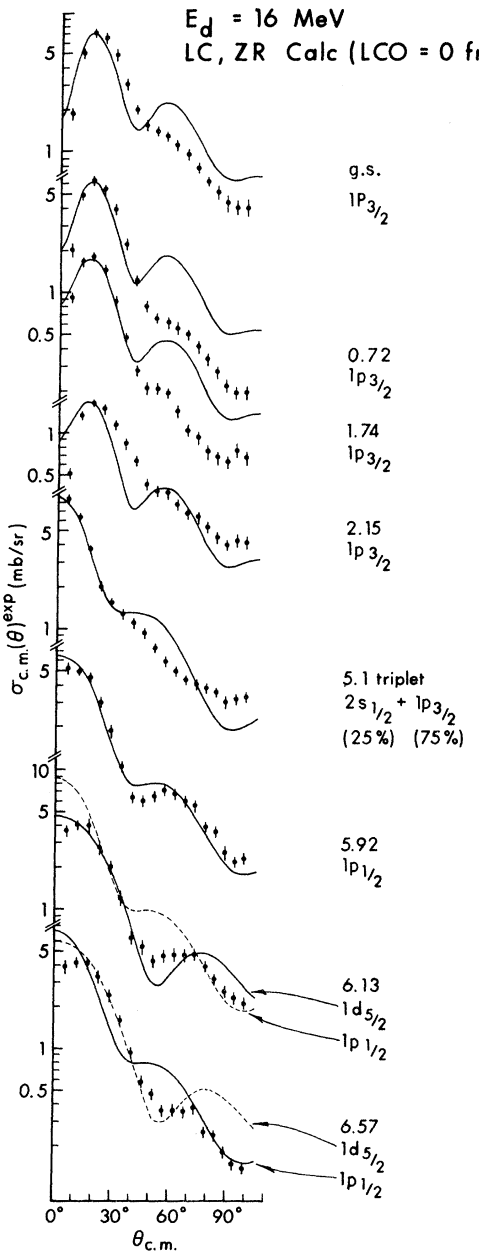

FIG. 7. Angular distributions for 16 MeV. See the caption for Fig. 5 for detail.

D. Absolute Cross-Section Errors

Relative cross sections were obtained on the basis of the elastic scattering monitored by the

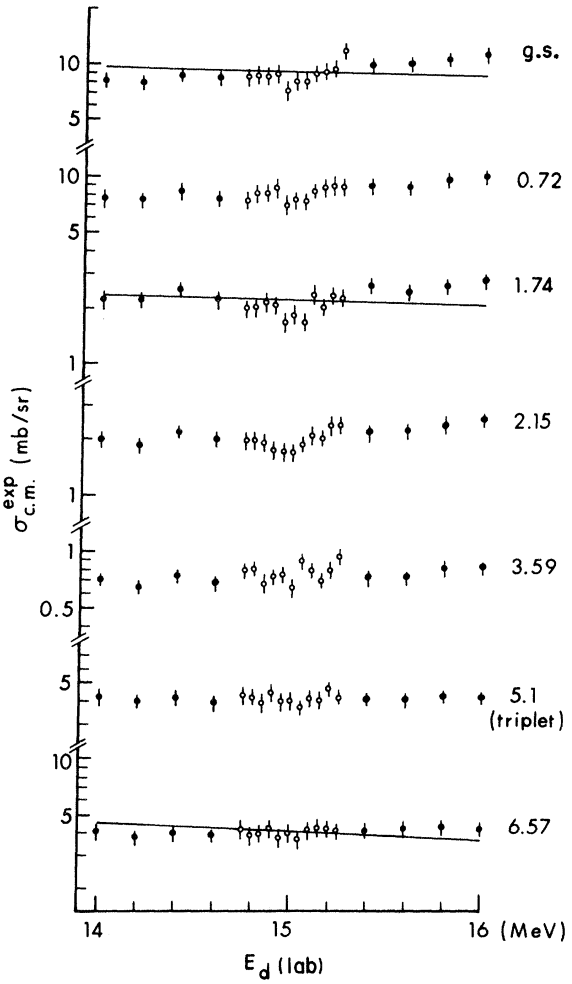

FIG. 8. Excitation functions for the ^{9}Be$(d, n)^{10}$B reaction measured at $\theta_{lab} = 15°$. Solid dots represent points measured with the thick target in steps of 200 keV, the open dots measured with the thin target in steps of 50 keV. Lines represent DWBA calculations, which were normalized to data arbitrarily.

surface-barrier detector (monitor normalization). Relative errors representing mainly counting statistics, background subtraction, and the error associated with the computer fitting procedure, are represented by vertical bars through the data points in Figs. 4–8. Absolute scales for the monitor-normalized relative cross sections were then fixed by fitting them to the absolute cross sections determined on the basis of the beam-charge times the target thickness (charge normalization).

The main contributions to the uncertainty in the absolute cross sections come from uncertainties in the target thickness (15%) and the neutron detector efficiencies (8%). In comparison, the other uncertainties of 1% on the beam-current integration and <2% on the detector solid angle are essentially negligible. The resulting over-all uncertainty on the absolute scale factor is $\leq 20\%$.

III. DWBA CALCULATIONS AND PARAMETER SENSITIVITIES

All the DWBA calculations were made with the code DWUCK.[23] The DWBA parameter-sensitivity study was focused mainly on the angular distribution for the ground-state transition at $E_d = 15$ MeV, for which the angular distributions were measured over a wide angular range ($5° \leq \theta_{lab} \leq 150°$). Consequently, detailed comparisons can be made between the calculated and measured angular distributions over the entire angular range.

A. Optical-Model Potentials

In view of reported difficulties in the deuteron optical-model potentials for light-mass nuclei, an extensive effort was made to study the effects of deuteron-potential sets on both the shape and magnitude of the calculated angular distributions. Various deuteron-potential sets were selected from recent literature which were appropriate for the present case. These sets are listed in standard notation in Table I. At the top of Fig. 9 the measured angular distribution is compared with the calculated ones based on these different sets. The solid line represents the calculation based on the deuteron set (V_d) used originally by Zeidman, Yntema, and Satchler in the analysis of the ^{10}B-$(d,p)^{11}$B reaction at 15.5 MeV,[24] and modified slightly by Smith and Ivash in the analysis of the same reaction.[25] The line represented by ×'s and the dashed line are based on the type I (Fitz-1) and type II (Fitz-2) potentials, respectively, determined from the ^{9}Be-d scattering at 11.8 MeV by Fitz, Jahr, and Santo.[26] The broken line is based on the set determined from the ^{9}Be-d scattering at 15.8 MeV by Cowley *et al.*[27] Finally, the line represented by dots is based on the Be set 2, determined from the ^{9}Be-d scattering with 12-MeV polarized deuterons by Griffith *et al.*[28] The neutron-potential set used in all cases is the set determined from the B-n scattering at 14 MeV by Frasca *et al.*[29] All the calculations shown at the

TABLE I. Optical-model-potential parameters used in the ^{9}Be$(d,n)^{10}$B DWBA calculations. All of the BRL sets were determined in a six-parameter-search procedure described in the text. The values of χ^2 are based on the data from Ref. 20.

		Real well parameters					Imaginary well parameters				
Set	Ref.	E (MeV)	U (MeV)	r_0 (fm)	a (fm)	U_{so} (MeV)	W_{vol} (MeV)	W_{surf} (MeV)	r_0' (fm)	a' (fm)	χ^2 (per point)
					Deuteron sets						
Zeidman	24	15.5	73.0	1.04	0.87	···	24.0	···	2.05	0.41	143
BRL-Zeidman	a	15.0	65.0	1.27	0.89	···	56.1	···	2.15	0.38	29
Fitz 1	26	11.8	118.0	0.869	1.01	6.0	···	6.87	1.68	0.879	82
BRL-Fitz 1	a	15.0	113.3	0.904	1.03	···	···	7.24	1.69	0.894	68
Fitz 2	26	11.8	78.0	0.967	1.04	6.05	30.0	···	1.07	0.870	62
BRL-Fitz 2	a	15.0	83.1	1.005	0.992	···	33.3	···	1.106	0.827	28
Cowley	27	15.8	65.0	1.250	0.790	···	···	7.20	1.250	1.025	45
BRL-Cowley	a	15.0	63.1	1.234	0.804	···	···	6.74	1.241	1.029	35
Griffith 2	28	12.0	100.0	1.070	0.890	8.57	···	20.4	1.100	0.590	127
BRL-Griffith 2	a	15.0	83.5	1.042	0.993	···	···	17.0	1.075	0.685	34
					Neutron sets						
Frasca	29	14.0	48.2	1.28	0.52	4.72	···	6.87	1.28	0.34	···
Wilmore-Hodgson	33		41.73	1.315	0.66	···	···	8.55	1.263	0.48	···
Lutz	34	14.0	42.36	1.35	0.55	5.0	···	9.44	1.35	0.36	···

[a] BRL sets determined by searching on the data from Ref. 20 with the preceding sets in the table used as start sets in the search.

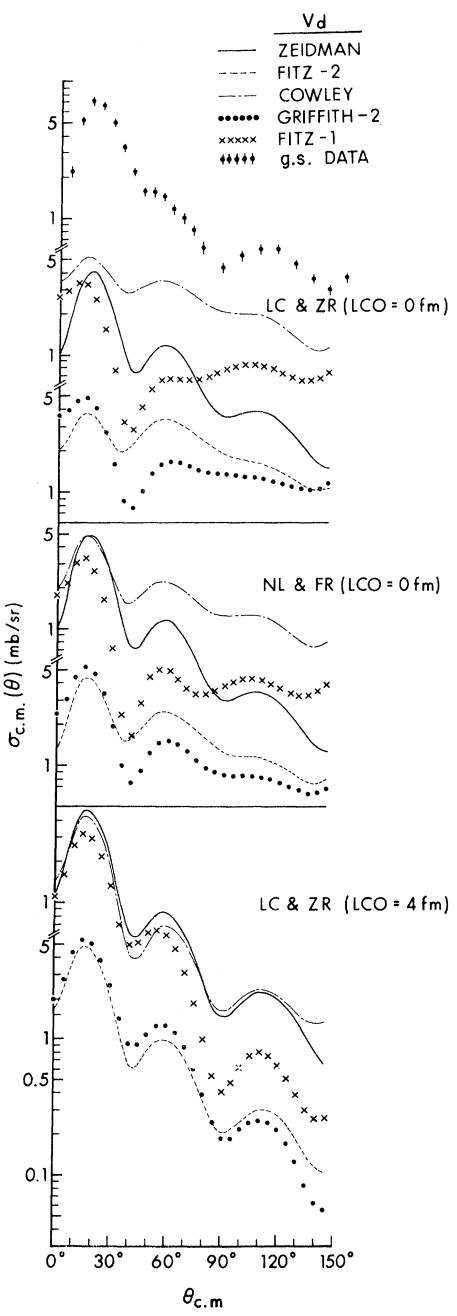

FIG. 9. Sensitivity of calculations as a function of deuteron optical-model potential sets. In all calculations, the same Frasca n set was used. The angular distribution at the very top represents the measured angular distribution for the ground-state transition at 15 MeV. The theoretical curves at the top represent noncutoff local zero-range DWBA calculations based on different d-potential sets represented by different curve patterns. The curves in the center show the effect of including nonlocality and finite-range corrections in the local zero-range calculations shown at the top. The curves at the bottom show the effect of introducing a lower cutoff of 4 fm in the local zero-range radial integrals.

top in this figure are noncutoff, local, zero-range calculations; the Woods-Saxon geometry for the form factor was fixed to the conventional value of $r_0 = 1.25$ fm and $a = 0.65$ fm, and the bound-state wave function was obtained for the $1p_{3/2}$ transfer.

It is immediately clear that Zeidman's is the only set which results in the calculation having the correct slope. It should be noted that the cross-section magnitude of the stripping peak varies from 3.6 to 5.2 mb/sr.

At the top of Fig. 10, the predictions of the four deuteron-potential sets used for the calculations shown in Fig. 9 are drawn in the same line con-

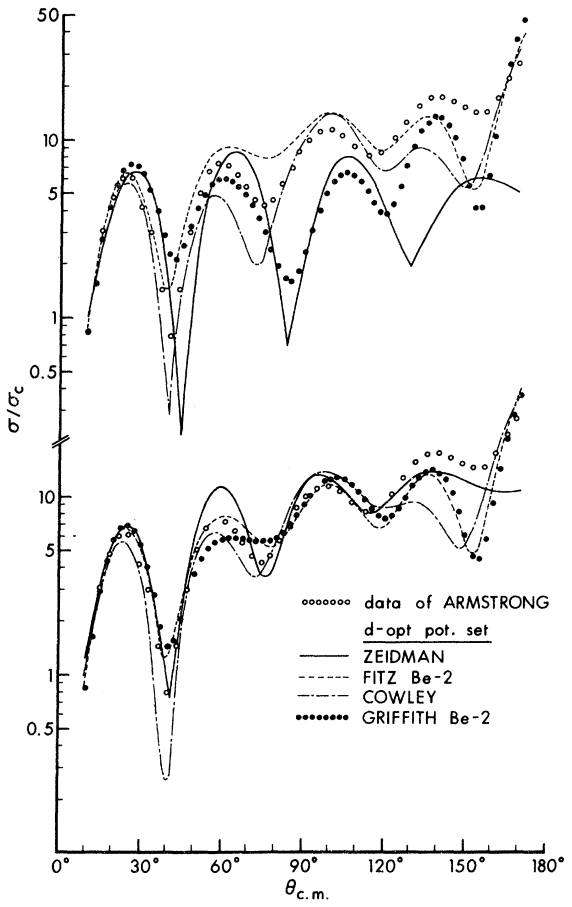

FIG. 10. At the top, comparison is made between the measured d elastic scattering of Ref. 20 represented by open dots and the optical-model predictions based on the different d-potential sets used in the DWBA calculations shown in Fig. 9. Note that the same curve conventions were used here as in Fig. 9 to represent the different d-potential sets. At the bottom, the same measured data is compared with new d sets obtained in this work via six-parameter searches with the use of the orginal d sets as start sets in the searches. Both types of d sets are listed in Table I. The spin-orbit potential was not included in the search.

ventions and compared with the ^{9}Be-d elastic angular distributions measured at 15 MeV by Armstrong *et al.*[20] represented by open circles. It is obvious that none of these sets are satisfactory.

At the bottom of Fig. 10, the same data are compared with predictions based on new parameter sets obtained at this laboratory with the optical-model potential-parameter-search code JIB.[30]

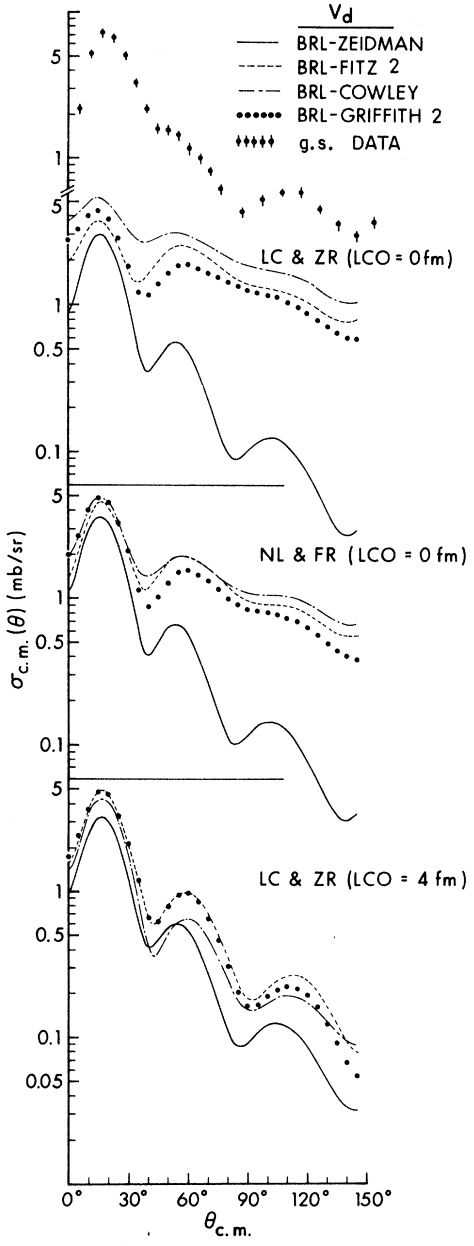

FIG. 11. Sensitivity of calculations as a function of the deuteron-potential sets obtained from the present work as shown at the bottom of Fig. 10. The calculational details and objectives are the same as in Fig. 9; see the caption for Fig. 9 for further details.

The original parameter sets used in generating the theoretical curves at the top of the figure were chosen as the start sets in the search. A six-parameter-search scheme was adopted in which only one parameter was allowed to vary at a time in the sequence of U, W, r_0, r_0', a, and a', while the other five remain fixed. The degrees of improvement in fits are shown quantitatively in Table I in the values of χ^2, in which the final sets obtained from the search are labeled as BRL-Zeidman set etc.

At the top of Fig. 11, the zero-range noncutoff DWBA calculations based on these new sets are compared with the data for the ^{9}Be$(d,n)^{10}$B ground-state transition. For consistency, the same notations as in Figs. 9 and 10 are used for designating the different sets in this figure. It is evident that no significant improvement in the DWBA calculations can be found with these modified deuteron-potential sets.

B. Effects of Nonlocality and Finite-Range Corrections and Lower Cutoffs

Zero-range DWBA calculations are not strictly valid when the angular momentum gap ΔL between the entrance- and exit-channel partial waves is not filled by the angular momentum transfer l.[31] A slight angular-momentum mismatch ($\Delta L = 2$) exists for the ^{9}Be(d,n) ground-state transition. Thus, inclusion of nonlocality and finite-range corrections into the zero-range calculations seems to be appropriate for the $l = 1$ ground-state transfer.

At the center of Fig. 9, the noncutoff calculations shown at the top are repeated with the finite-range and nonlocality corrections based on the local-energy approximation (LEA).[32] The standard values of $\beta_{NL}^{d} = 0.54$, $\beta_{NL}^{n} = 0.85$, and $R_{FN} = 0.62$ are used in all. Likewise, the calculations based on the different deuteron-parameter sets shown at the top of Fig. 11 are repeated with the corrections included at the center of Fig. 11. As can be seen, the corrections tend to bring the slopes of the curves more into agreement with the data, but the effect is obviously not large enough. The calculations based on the Zeidman and BRL-Zeidman sets still remain the only realistic ones although the magnitude of the peak cross sections increases by 20% with the corrections.

At the bottom of Figs. 9 and 11, the zero-range noncutoff calculations shown at the top of these figures are repeated with the inclusion of a lower cutoff of 4 fm in the radial integrals. It is remarkable that all the curves previously unacceptable appear now to reproduce rather well the shape of the measured angular distribution shown at the top. The fact that the use of such a sharp cutoff improves the calculations so drastically usually im-

plies that the contribution from the nuclear interior to the radial integral has been overestimated in the conventional DWBA calculations. It is clear, however, that the suppression of the contribution from the nuclear interior alone is not sufficient for generating realistic calculations. This is because, first, the nonlocality and finite-range correction affected the shape of the angular distribution very little and, secondly, the 4-fm cutoff is much larger than the nuclear radius of ~2.7 fm. It is not surprising to observe that the calculations with the Zeidman set are the only acceptable calculations in the zero-range form without the use of any cutoffs, because the Zeidman set is the only one modified to fit the measured (d, p) angular distributions in Ref. 24.

At the top of Fig. 12 three local, zero-range calculations based on three different deuteron sets are compared with each other and the measured angular distributions at 15 MeV for $l=1$ transitions to the three lowest states in ^{10}B. The solid, dashed, and broken curves represent the calculations based on the Zeidman set without a lower cutoff (LCO), the Fitz set 2 with LCO = 4 fm and the BRL-Fitz set 2 with LCO = 4 fm, respectively. The cross-section scale refers to the DWUCK calculations, to which the data are arbitrarily normalized. It should be noted that the calculations consistently overestimate the second maximum at ~60° for the $l=1$ transfers.

At the bottom of the figure the sensitivity of the noncutoff, local, zero-range calculations due to the neutron optical-potential-parameter sets is exhibited. Zeidman's deuteron set was used in all cases. The solid curve represents the calculation based on the neutron set determined from the B-n scattering at 14 MeV by Frasca *et al.*[29]; the dashed curve represents the Wilmore-Hodgson energy-dependent global set[33]; and the broken curve represents the set determined from the ^{10}B-n scattering at 14 MeV by Lutz, Mason, and Karvelis.[34] Again the data for the ground-state transition are normalized to the curves arbitrarily. It is clear that the calculations are not very sensitive to the choice of neutron sets.

C. Reanalysis of the ^{9}Be(^{3}He,d)^{10}B Data at 17 MeV

In view of the difficulties encountered in the DWBA calculations on the (d, n) reaction, it was felt worthwhile to investigate the quality of DWBA fits in the ^{9}Be(^{3}He, d)^{10}B reaction. The most frequently quoted work on this reaction in connection with the discrepancy in the $T=1$ S_{rel} in recent years is the paper by Siemssen *et al.*[1] Unfortunately, no DWBA calculations are shown in Ref. 1. Thus, we decided to reanalyze the data reported in Ref. 1 with DWBA calculations based on realistic parameter sets found in the literature.

In Fig. 13, the measured (^{3}He, d) angular distributions at 17 MeV for transitions to the first four states in ^{10}B are compared with the noncutoff, local, zero-range calculations represented by

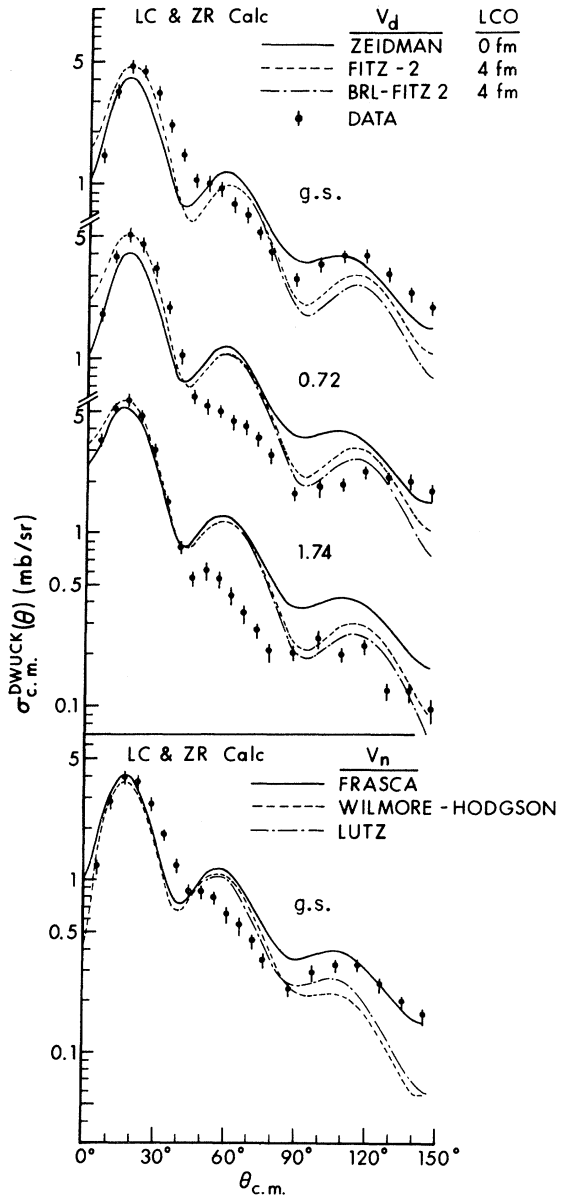

FIG. 12. At the top, three different local zero-range DWBA calculations based on three different d sets are compared with the measured angular distributions for the first three low-lying states, which are normalized to the theoretical ones arbitrarily. In all calculations the same Frasca n set was used. At the bottom, the sensitivity of calculations as a function of neutron-potential sets is indicated; again the data are normalized to the theoretical curves arbitrarily.

curves. All the transitions have been assumed to be $1p_{3/2}$ transfers. The ^{3}He set is the ^{9}Be-^{3}He set at 18 MeV determined by Park *et al.*,[35] and the deuteron set is the Zeidman set[24] used in the (d,n) calculations earlier. As can be seen, the quality of the fits is remarkable except perhaps for the 1.74-MeV transition. Calculations including the LEA nonlocality and finite-range corrections were also tried, but no discernible change in shape could be observed. The corrections, however, enhance the cross-section magnitudes by as much as 30%. The effects of using different ^{3}He and d sets were also examined. The use of the ^{3}He set with $U=161$ MeV obtained by Crosby and Legg[4] from the ^{9}Be-^{3}He scattering at 10 MeV sharpens the structure of the second stripping peak but reduces the cross-section magnitudes of the first stripping peak by as much as 26%. The use of the Fitz-2-d set[26] in place of the Zeidman set, for instance, broadens the structure of the second peak but increases the cross section by as much as 50% in contrast to the ^{3}He case. In either case, the shape of the stripping peak remains the same, so that there exists no ambiguity in the fitting procedure for extracting spectroscopic factors.

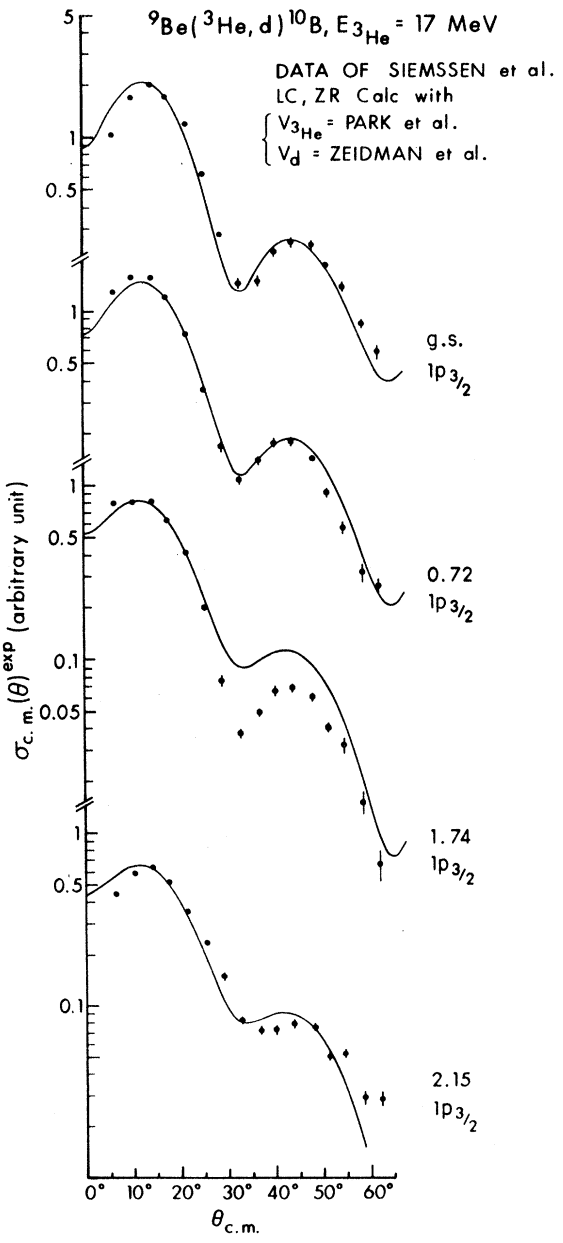

FIG. 13. Results of the reanalysis of the ^{9}Be(^{3}He, d)^{10}B reaction data measured at 17 MeV by Siemssen *et al.* (Ref. 1). The curves represent local zero-range DWBA calculations without the use of a lower cutoff. Note the imperfect fit for the $T=1$ 1.74-MeV transition.

One immediately relevant question is why the DWBA predictions for the ^{9}Be(^{3}He, d)^{10}B reaction are superior to those for the ^{9}Be$(d,n)^{10}$B reaction. It is well known that (^{3}He, d) reactions are surface reactions for which the contributions to the reaction amplitude are well localized in angular-momentum space. The amplitude is dominated by a few partial waves on the nuclear surface. In such a case the conventional DWBA method is known to be valid.[31] A more favorable situation with (^{3}He, d) arises also from consideration of the reaction mechanism. The 17-MeV ^{3}He incident energy feeds levels at as high as 43 MeV excitation in the ^{9}Be + ^{3}He compound nucleus, more than 10 MeV higher than in the ^{9}Be + d compound nucleus when $E_d=15$ MeV. The higher level density in the ^{12}C compound nucleus assures a better overlapping of compound resonances, so that the averaging requirement inherent to the optical-model potentials is more properly met for the ^{9}Be + ^{3}He channel than for the ^{9}Be + d channel.[36] Furthermore, emission of neutrons by evaporation in (d,n) is expected to be more severe than the emission of deuterons in (^{3}He, d). In short, the DWBA analysis of the (^{3}He, d) reaction is likely to be more successful than that of the (d,n) reaction for the energy range of interest.

IV. SPECTROSCOPIC FACTORS

The absolute spectroscopic factors (S_{abs}) were extracted via the relation:

$$\left(\frac{d\sigma}{d\sigma}\right)^{exp} = NC^2S\,\frac{2J_f+1}{2J_i+1}\,\frac{2s+1}{2(2j+1)}\left(\frac{d\sigma}{d\Omega}\right)^{DWUCK} \text{ mb/sr}, \quad (2)$$

where J_i and J_f are the initial and final state spins; s and j are the spin and total angular momentum of the transferred nucleon. The value of

TABLE II. Absolute spectroscopic factors for levels in ^{10}B from the ^{9}Be(d,n) reactions and from theory.

			^{9}Be$(d,n)^{10}$B					Theory			
								Cohen-Kurath [a]		Varma [b]	
E_x (MeV)	$J^\pi T$	nlj	E_D (MeV) 7.0 [c]	7.0 [d]	12.0 [d]	15.0 [d]	16.0 [d]	E_x (MeV)	S_{abs}	E_x (MeV)	S_{abs}
0.00	$3^+,0$	$1p_{3/2}$	0.98	1.14	1.15	1.28	1.33	0.00	1.20	0.00	0.76
0.72	$1^+,0$	$1p_{3/2}$	2.24	2.22	2.35	2.62	2.42	0.90	1.35	0.47	0.99
1.74	$0^+,1$	$1p_{3/2}$	1.00	1.31	1.59	1.97	1.78	1.42	2.36	1.79	0.98
2.15	$1^+,0$	$1p_{3/2}$	0.40	0.54	0.49	0.55	0.50	2.38	0.73	2.43	0.46
3.59	$2^+,0$	$1p_{3/2}$	0.44		0.12	0.12		3.34	0.39	3.87	0.06
4.77	$3^+,0$	$1f_{7/2}$	0.42					4.72	0.012		
5.11	$(2)^-,0$	$2s_{1/2}$	1.28		0.20	0.18	0.15			5.21	0.10
5.17	$2^+,0$	$1p_{1/2}$			0.60	0.55	0.44	5.58	0.274		
5.92	$2^+,0$	$1p_{1/2}$	1.32		0.68	0.65	0.49	5.53	0.428		

[a] See Ref. 16.
[b] See Ref. 17.
[c] See Ref. 2.
[d] Present work.

C^2, where C is the isospin Clebsch-Gordan coefficient, is equal to $\frac{1}{2}$ in the case of the ^{9}Be(d,n) reaction. The normalization constant[37] used here is $N = 1.65 \times 10^4$ MeV^2 fm^3, which is based on the Hulthèn wave function for the deuteron.

The values of S_{abs} were extracted from fitting the calculated cross sections to the measured angular distributions at the stripping maxima. The fits are shown in Figs. 4–7, in which the noncutoff, local, zero-range calculations represented by curves are based on the combination of the Zeidman d set and the Frasca n set. The bound-state wave functions were generated in the standard separation-energy prescription with the Woods-Saxon well geometry of $r_0 = 1.25$ fm and $a = 0.65$ fm; the Thomas-type spin-orbit coupling with $\lambda = 25$ was included in all the calculations. In most calculations the $1p_{3/2}$ orbit was chosen arbitrarily for $l = 1$ transfers, as the correct j assignments for the $l = 1$ transfers neither have been known from literature nor can be made in the present work, primarily due to lack of the j dependence in the ^{9}Be$(d,n)^{10}$B angular distributions.

In spite of the fact that the Zeidman d set compares poorly with the measured elastic scattering angular distribution at 15 MeV as shown in Fig. 10, this set was chosen for all the calculations fitted to the data in Figs. 4–7 because it was the only set which resulted in calculations having nearly correct shapes of the measured angular distributions without the use of lower cutoffs and nonlocality and finite-range corrections. Depen-

TABLE III. Comparison of relative spectroscopic factors for levels in ^{10}B from the present ^{9}Be(d,n) study with those from the previous (d,n) and $(^3$He$,d)$ works and theory.

			^{9}Be$(d,n)^{10}$B						^{9}Be$(^3$He$,d)^{10}$B		Theory	
			Previous work		Present work				$E_{^3\text{He}}$ (MeV)			
E_x [a] (MeV)	J^π, T	l_p	E_D (MeV) 5.5 [b]	7.0 [c]	7.0	12.0	15.0	16.0	10.0 [d]	17.0 [e]	Cohen [f]	Varma [g]
0.00	$3^+,0$	1	1.0	1.0	1.0	1.0	1.0	1.0	1.0	1.0	1.0	1.0
0.72	$1^+,0$	1	2.98	2.3	1.94	2.04	2.05	1.82	1.8	1.8	1.12	1.30
1.74	$0^+,1$	1	1.45	1.0	1.14	1.38	1.54	1.34	2.6	2.6	1.96	1.29
2.15	$1^+,0$	1	0.46	0.41	0.48	0.42	0.43	0.38	0.71	0.55	0.61	0.61
3.59	$2^+,0$	1	0.24	0.45		0.11	0.09		0.30		0.33	0.08
4.77	$3^+,0$	1	0.07						0.15		0.01	
		2	0.36	0.43								
5.11	$(2)^-,0$	0	0.39	1.3		0.17	0.14	0.11				0.13
5.17	$2^+,1$	2	0.49			0.52	0.43	0.34			0.23	
5.18	$1^+,0$	1										
5.92	$2^+,0$	1	0.59	1.3		0.59	0.51	0.37	1.2		0.36	

[a] See Ref. 12.
[b] See Ref. 3.
[c] See Ref. 2.
[d] See Ref. 4.
[e] See Ref. 1.
[f] See Ref. 16.
[g] See Ref. 17.

dence of the S_{abs} values on the DWBA parameters will be examined later.

In Table II the S_{abs} values obtained from this work are compared with those from the previous ^{9}Be(d,n) work at 7 MeV[2] and two independent theoretical predictions.[16,17] The poor agreements among these different sources are expected because the extracted S_{abs} values depend on the choice of the normalization constant N in (2) and more importantly on the choices of the DWBA parameters. Thus, a more meaningful comparison can be made on the relative spectroscopic factors (S_{rel}). In Table III the S_{rel} values, obtained by normalizing the $T=0$ ground-state spectroscopic factors to 1, are shown for the (d,n), (^{3}He, d), and theoretical works. Columns 4 and 5, respectively, list the (d,n) values obtained at 5.5 MeV by Fife, Neilsen, and Dawson,[3] and at 7.0 MeV by Buccino and Smith.[2] In columns 6–9 the (d,n) values from the present work are listed for the four different deuteron energies. Columns 10 and 11 list the (^{3}He, d) values obtained at 10 MeV by Crosby and Legg[4] and obtained at 17 MeV by Siemssen *et al.*[1] The last two columns list the theoretical values of the shell-model calculations by Cohen and Kurath[16] and the independent calculations by Varma and Goldhammer.[17]

V. DISCUSSION

A. Spectroscopic Factors

The most important observation to be made from Table III is that there exist a wide range of S_{rel} values for the $T=1$ 1.74-MeV state. The previous conclusion by Siemssen *et al.*[1] that the $T=1$ S_{rel} value in (d,n) is less than in (^{3}He, d) by as much as a factor of 3 was made primarily on the basis of the (d,n) S_{rel} value of Buccino and Smith[2] and of the (^{3}He, d) value of Siemssen *et al.*[1] It is important to notice that the S_{rel} value of 1.0 at 7 MeV from Ref. 2 is reproduced neither by the (d,n) work at 5.5 MeV of Ref. 3 nor by the present (d,n) work at higher energies. From the present work there seems to be a definite energy dependence of the $T=1$ S_{rel} in that it increases almost systematically as the incident deuteron energy increases (save the data at 16 MeV, for which the S_{rel} values are consistently lower for the rest of the $T=0$ states). Our 15-MeV value of 1.53 is in closer agreement with the value 1.96 of Cohen and Kurath[16] than the (^{3}He, d) value of 2.6. Other noticeable discrepancies between Ref. 2 and the present work are the S_{rel} values for the $T=0$ states at 5.11 and 5.92 MeV. Our values are in closer agreement with theoretical predictions.

Uncertainties in the spectroscopic factors due to ambiguities in the DWBA analysis should be considered. In Table IV the effects of changing parameters in DWBA calculations on spectroscopic factors are shown for the ^{9}Be(d,n) reaction at 15 MeV. Inclusion of nonlocality and finite-range corrections into the noncutoff zero-range calculations reduces the S_{abs} values by 17% but does not change S_{rel}. The choice of a different Woods-Saxon well geometry in the calculations increases S_{abs} by approximately 6%, but lowers the $T=1$ S_{rel} by only 3%. The use of another deuteron set, say that of Fitz 2, but with a lower cutoff of 4 fm, reduces S_{abs} by 10–15%, but increases the $T=1$ S_{rel} by 8%. Thus the over-all error associated with the S_{rel} values from the present ^{9}Be(d,n) measurements (listed in Table III) does not exceed ±10%. Realistic limits on the errors in the absolute spectroscopic factors given in Table II, however, are hard to determine from this work. Beyond the estimated uncertainties of ±20% in the DWBA calculations, there are additional uncertainties associated with an alternative choice of the (d,n) normalization constant N, the compound contribution, ambiguities in the fitting procedure and, more significantly, the absolute scale error in the measured cross sections.

Table V summarizes the results of the reanalysis of the ^{9}Be(^{3}He, d) data at 17 MeV from Ref. 1. The consistency of the S_{rel} values was tested with the use of four different ^{3}He and d potential sets. It should be noted that the S_{rel} value of the $T=1$ state is ~2.4 compared to 2.6 obtained by Siemssen *et al.*[1] However, it is clear that, in general the (^{3}He, d) values are less sensitive to the DWBA parameters than the (d,n) values.

B. Isospin Dependence

There have been numerous theoretical efforts to resolve the discrepancies in S_{rel} values for $T=1$ states between (d,n) and its companion (^{3}He, d). Fuchs and Santo[38] focused their interest on a difference in angular-distribution shape between the ground-state ($T=0$) and 1.74-MeV state ($T=1$)

TABLE IV. Dependence of spectroscopic factors for the ^{9}Be$(d,n)^{10}$B reaction, E_d =15 MeV, on DWBA parameters. In all calculations the Frasca n set (Ref. 29) was used.

		V_d = Zeidman[a] NLFR		Fitz 2[b] LZR, LCO = 4 fm		Zeidman LZR; r_0 = 1.32, a = 0.57	
E_x (MeV)	J^π, T	S_{abs}	S_{rel}	S_{abs}	S_{rel}	S_{abs}	S_{rel}
0.00	$3^+, 0$	1.06	1.0	1.08	1.0	1.38	1.0
0.72	$1^+, 0$	2.18	2.06	2.27	2.09	2.78	2.01
1.74	$0^+, 1$	1.63	1.54	1.80	1.66	2.06	1.49
2.15	$1^+, 0$	0.46	0.44	0.51	0.47	0.58	0.42

[a] See Ref. 24.

[b] See Ref. 26.

TABLE V. Relative spectroscopic factors from the ^{9}Be(^{3}He, d)^{10}B reaction based on the data from Ref. 1 and DWBA calculations made with different combinations of the ^{3}He- and d-potential sets. The calculations are noncutoff local zero-range calculations unless specified otherwise.

E_x (MeV)	J^π, T	$V_{^3\mathrm{He}}$ (Park) [a] + V_d (Zeidman) [d]	Park [b] + Zeidman	Park + Fitz 2 [e]	Park + BRL-Fitz 2 [f]	Crosby [c] + Ziedman
0.00	$3^+, 0$	1.00	1.00	1.00	1.00	1.00
0.72	$1^+, 0$	1.77	1.78	1.77	1.76	1.76
1.74	$0^+, 1$	2.44	2.45	2.40	2.40	2.36
2.15	$1^+, 0$	0.60	0.60	0.60	0.60	0.57

[a] See Ref. 35.
[b] Finite-range nonlocality correction included in DWBA calculations.
[f] This work.
[d] See Ref. 24.
[e] See Ref. 26.
[c] See Ref. 4.

transitions in both (d, n) and $(^3\mathrm{He}, d)$: The angular distribution for the $T=1$ state falls more rapidly than that for the $T=0$ ground state. This phenomenon has also been observed with consistency for all the incident deuteron energies in the present (d, n) reaction as can be seen in Figs. 4–7. They indicated the possible connection between the isospin dependence of angular-distribution shape and the $\vec{t} \cdot \vec{T}$ term of the Lane potential in the nucleon-nucleus potentials. Some effort has been made by Tamura[9] to resolve this discrepancy by including charge-exchange coupling between (d, p) and (d, n) channels in coupled-channel DWBA calculations. Final results of the calculations showed that the ^{9}Be$(d, n)^{10}$B cross section for the $T=1$ transition was increased by a factor of 1.35 in the wrong direction and thus they were forced to conclude that the charge-exchange process was insufficient to give the desired results.[10]

More recently, Robson and Cotanch[11] have been working on the problem with a different approach. The idea of the charge-exchange process was represented by the isospin dependence of distorted waves and form factors. They point out that the T-structure of the (d, n) reaction is different from that of $(^3\mathrm{He}, d)$. Both $T=0$ and $T=1$ excitations in $(^3\mathrm{He}, d)$ are selective (or singly forbidden); in (d, n) the $T=0$ excitation is a singly allowed reaction, whereas the $T=1$ excitation is selective. Based on these different classifications, their preliminary conclusion is that the discrepancy in S_{rel} value virtually disappears. Final results have not been published as yet.

C. l_p Assignments of Some Levels

Since the J^π assignments are known for most of the levels below 7 MeV excitation in ^{10}B and the main goal of the present study was not focused on J^π or l_p assignments, discussions will be limited to the levels under controversy. Most of the levels in ^{10}B are associated with an $l_p=1$ transfer in the ^{9}Be$(d, n)^{10}$B reaction as can be seen in Figs. 4–7. The usefulness of the (d, n) reaction as a spectroscopic tool for J^π assignments is severely limited by the non-zero target spin and the failure to recognize the j dependence for an $l=1$ transfer in the present (d, n) angular distributions, as can be seen in Fig. 6. The DWBA calculations (represented by curves in these figures) made for $1p_{3/2}$ transfers could be replaced by $1p_{1/2}$ transfers or vice versa in all of the $l=1$ transfers. In fact the shell-model calculations of Cohen and Kurath[16] predict that both $1p_{3/2}$ and $1p_{1/2}$ single-particle strengths are highly fractionated all the way up to 28 MeV excitation. This is also supported by the sum rule applied to the S_{abs} values in Table II. The sum rule in single-proton transfer (stripping) is given in terms of the target isospin T by

$$P_j = \frac{2T}{2T+1} \sum_f \frac{2J_f+1}{2J+1} S_{f>} + \frac{1}{2T+1} \sum_f \frac{2J_f+1}{2J+1} S_{f<} \tag{3}$$

for a given shell-model orbit j.[39] Here P_j is the occupation number; J and J_f are the spins of the target and final state; and $S_>$ and $S_<$ are the S values for $T_f = T \pm \frac{1}{2}$. Assuming that all the $l=1$ transfers were $1p_{3/2}$ transfers and applying Eq. (3) to the 15-MeV data in Table II, we would obtain 3.38, which is still short of the total $p_{3/2}$ strength available.

3.59-MeV level. The previous (d, n) works at 5.5 MeV[3] and 7 MeV[2] assigned an $l=1$ to this transition although the measured angular distributions were hardly reproduced by the calculations. The measured angular distributions at 12 and 15 MeV from the present work (Figs. 5 and 6) have too

flat a slope compared with the $l=1$ calculations. An admixture of $1f_{7/2}$ calculation into the $1p_{3/2}$ calculation, represented by dashed lines in Figs. 5 and 6, greatly improves the quality of fit. If taken seriously, the $p_{1/2,3/2}+f_{7/2}$ mixture would narrow the J^{π} limit to $2^{+}(3^{+})$, which is in agreement with the 2^{+} assignment given in Ref. 12.

4. 77-MeV level. This level is very weakly populated and not well resolved from the ground state of ^{13}N populated by the (d,n) on ^{12}C contaminant as can be seen in Fig. 2. The angular distribution is compared with $1f_{7/2}$ transfer in Fig. 5. It is possible to improve the quality of fit by adding $1p_{3/2}$ as in the case of the 3.59-MeV level. The $l=1$ assignment made by Crosby and Legg[4] in $(^{3}\mathrm{He},d)$ is not convincing. Cohen and Kurath predict a 3^{+} state at 4.72 MeV, which is in support of our $1f_{7/2}$ $(+1p_{3/2})$ assignment for the transition.

5. 1-MeV triplet. The combined angular distribution of the triplet consisting of the 5.11-, 5.16-, and 5.18-MeV levels is reasonably well compared with the same amount of admixture of $2s_{1/2}$ and $1p_{3/2}$ transfers for all three energies as shown in Figs. 5–7. It is thus in agreement with the previous (d,n) works. The question as to whether the 5.18-MeV level is populated in (d,n) of course cannot be answered here because of the lack of necessary energy resolution.

5. 92-MeV level. A remarkably good fit is obtained for the $l_p=1$ transition to the 5.92-MeV level as seen in Figs. 5–7. Both $1p_{1/2}$ and $1p_{3/2}$ calculations are compared with the measured angular distribution for the 15-MeV data in Fig. 6. The $l_p=1$ j dependence in DWBA calculations again is not distinctive. Cohen and Kurath predict a 2^{+}, $T=0$ state at 5.53 MeV and a 2^{+}, $T=1$ state at 5.58 MeV. It is not clear which of these corresponds to the 5.92-MeV level populated in (d,n).

6. 03-MeV level. Fife, Neilson, and Dawson[3] reported the population of this level in their (d,n) work. It is not confirmed here.

6. 13-MeV level. The most controversy arises for the J^{π} assignment of this level. Young, Lindgren, and Reichart[13] from the ^{11}B$(^{3}\mathrm{He},\alpha)^{10}B(\alpha_0)^{6}$Li correlation and Meyer, Pixley, and Truol[14] from the ^{6}Li-α scattering assign 3^{-} to this level. On the other hand, the $(^{3}\mathrm{He},d)$ works by Forsyth, Knudson, and Young[15] and by Crosby and Legg[4] propose a positive-parity state. None of the previous (d,n) works were able to assign a definite l_p value. The calculations representing both the $1d_{5/2}$ transfer and the $1p_{1/2}$ transfer are compared with the measured angular distributions in Figs. 5–7. Extreme care was exercised in making the DWBA calculations for these transitions due to the fact that the binding energy of the transferred proton corresponding to these transitions is merely $\sim\frac{1}{2}$ MeV. In order to guarantee the normally desired asymptotic behavior of the form factor, the upper cutoff for the radial integral was extended to 60 fm. The 15- and 16-MeV data agree better with the $1d_{5/2}$ calculation than with the $1p_{1/2}$. Thus, we favor the negative-parity assignment. However, the shell-model calculation predicts the 1^{+} assignment at a level at 6.19 MeV, which would point to the $l_p=1$ assignment for the 6.13-MeV level in the present (d,n) work.

6. 35-MeV level. The only source which claims the definite population of this level is the (d,n) work by Buccino and Smith.[2] Even in that work the proposed level is completely overlapped with the neutron group from the ^{16}O$(d,n)^{17}$F$_{0.5}$ reaction. The existence of this level cannot be confirmed from the present (d,n) measurement primarily due to the presence of ^{16}O contaminant in the target.

6. 57-MeV level. A situation similar to that for the 6.13-MeV level occurs here. The $(^{3}\mathrm{He},\alpha)$ correlation and ^{6}Li-α scattering experiments propose a negative-parity assignment for this level, while the $(^{3}\mathrm{He},d)$- and (d,n)-proton-transfer-reaction works prefer a positive-parity assignment. The measured angular distributions corresponding to this transition for 12, 15, and 16 MeV all show a close resemblance to those of the 6.13-MeV transition. Again, both the $1d_{5/2}$ and $1p_{1/2}$ calculations are compared with the data in Figs. 5–7. Judging strictly from the stripping-peak fits, the $l_p=2$ assignment is favored, but the $l_p=1$ assignment cannot be ruled out completely.

VI. CONCLUSIONS

Conventional DWBA calculations for the ^{9}Be(d,n)-^{10}B reaction at 12, 15, and 16 MeV were satisfactory in predicting the structure of stripping peaks in the measured angular distributions for transitions to most of the levels below 6.57 MeV excitation in ^{10}B. Although the gross structure of the measured angular distributions beyond the stripping peaks were correctly predicted by the calculated ones, the detailed structure of the former was far from reproduced by the latter (except perhaps for the transition to the 5.92-MeV level). It was found that deuteron optical-model potentials extracted directly from elastic scattering data lead to angular distributions with unrealistic slopes in DWBA calculations. All the deuteron sets became acceptable only when a lower cutoff as large as 4 fm is introduced in the radial integrals.

The abnormally flat angular distribution for the 3.59-MeV transition, assigned as an $l=1$ transfer in previous (d,n) and $(^{3}\mathrm{He},d)$ works, was well reproduced by a mixture of $p_{1/2,3/2}$ and $1f_{7/2}$ in the present (d,n) work. The question of the correct

parity assignments for the 6.13- and 6.57-MeV levels could not be answered unambiguously from this study because of non-uniqueness in DWBA fits. Nevertheless, we favor tentatively the negative-parity assignment as explained in the text.

The j dependence associated with $l=1$ transfers was not recognized to a measurable degree in the present (d,n) transitions.

The previously reported discrepancy in relative spectroscopic factors between (d,n) and $(^3\mathrm{He},d)$ leading to states with different isospin within the same final nucleus ^{10}B was confirmed from the present investigation. However, it should be pointed out that the extent of the discrepancy was not found to be as large as it had been previously reported—a factor of <2 instead of ~3. More significantly, there seems to be a systematic increase in S_{rel} values for the $T=1$ 1.74-MeV state as the incident deuteron energy increases. Thus we conclude that the final confirmation of the discrepancy between (d,n) and $(^3\mathrm{He},d)$ reactions cannot be established until the (d,n) experiment is studied at much higher energies at which the interference from the compound-nucleus mechanism can be safely ignored.

Further refinement in the conventional zero-range DWBA formalism seems to be in order. Inclusion of such effects as the two-step process, the recoil effect, and the D component in the deuteron wave function into the present calculations may be essential to explain the phenomenon observed in the experiments. The recent attempt by Cotanch and Robson[11] to resolve the (d,n) and $(^3\mathrm{He},d)$ discrepancy with DWBA calculations constructed on the basis of the isospin formalism is very encouraging and we look forward to their final results.

It would also be interesting to see if the energy dependence in the $T_>$ relative spectroscopic factors persisted in other light odd-odd nuclei where the discrepancy between (d,n) and $(^3\mathrm{He},d)$ reactions has also been reported previously.

Finally, the theoretical spectroscopic factors, based on the shell-model calculations of Cohen and Kurath[16] and, more recently, calculated by Varma and Goldhammer,[17] are generally in poor agreement with those extracted from the present work.

ACKNOWLEDGMENTS

The authors are grateful to Dr. D. Eccleshall for suggesting and encouraging this study. We are indebted to Dr. C. E. Hollandsworth and Dr. W. P. Bucher for their assistance in the initial phase of the setup. We are obliged to Dr. H. D. Jones for his assistance on the SEL-86 computer, J. Smith and D. E. Bainum for their assistance in data analysis, and J. A. Morrissey for his service in accelerator operation.
One of us (YSP) enjoyed informative discussions with Professor W. W. Daehnick and Professor R. M. Drisko. Finally, we thank Dr. S. G. Buccino for his careful reading of the manuscript.

---

*Present address: Nuclear Structure Laboratory, University of Rochester, Rochester, N.Y. 14627.

[1]R. H. Siemssen, G. C. Morrison, B. Zeidman, and H. Fuchs, Phys. Rev. Lett. 16, 1050 (1966).
[2]S. G. Buccino and A. B. Smith, Phys. Lett. 19, 234 (1965).
[3]A. A. Fife, G. C. Neilson, and W. K. Dawson, Nucl. Phys. A91, 164 (1967).
[4]M. A. Crosby and J. C. Legg, Nucl. Phys. A95, 639 (1967).
[5]More recently by H. G. Bingham, J. E. Holden, and H. T. Fortune, Bull. Am. Phys. Soc. 16, 621, (1971); and private communication with Dr. Fortune and Dr. Holden.
[6]G. S. Mutchler, D. Rendic, D. E. Velkley, W. E. Sweeney, Jr., and G. C. Phillips, Nucl. Phys. A172, 469 (1971).
[7]J. P. Schiffer, G. C. Morrison, R. H. Siemssen, and B. Zeidman, Phys. Rev. 164, 1274 (1967).
[8]R. G. Couch, F. G. Perey, J. A. Biggerstaff, and K. K. Seth, Phys. Lett. 29B,657 (1969).
[9]T. Tamura, Phys. Rev. Lett. 19, 321 (1967); Phys. Rev. 165, 1123 (1868).
[10]R. Coker and T. Tamura, Phys. Rev. 182, 1277 (1969).
[11]S. Cotanch and D. Robson, Bull. Am. Phys. Soc. 17, 510 (1972); Phys. Rev. C 7, 1714 (1973); private communication with Dr. Robson.
[12]T. Lauritsen and F. Ajzenberg-Selove, Nucl. Phys. 78, 1 (1966).
[13]F. C. Young, R. A. Lindgren, and W. Reichart, Nucl. Phys. A176, 289 (1971).
[14]V. Meyer, R. E. Pixley, and P. Truol, Nucl. Phys. A101, 321 (1967).
[15]P. D. Forsyth, A. R. Knudson, and F. C. Young, Nucl. Phys. 85, 153 (1966).
[16]S. Cohen and D. Kurath, Nucl. Phys. A101, 1 (1967).
[17]S. Varma and P. Goldhammer, Nucl. Phys. A125, 193 (1969).
[18]P. Goldhammer, J. R. Hill, and J. Nachamkin, Nucl. Phys. A106, 62 (1968).
[19]Preliminary results of this study by the authors appeared in Bull. Am. Phys. Soc. 16, 1186 (1971).
[20]D. D. Armstrong, J. G. Beery, P. W. Keaton, Jr., and L. R. Veeser, Los Alamos Scientific Laboratory Report No. LA-4177, 1969 (unpublished).
[21]J. E. Brolley, Jr., T. M. Putnam, and L. Rosen, Phys. Rev. 107, 820 (1957).
[22]J. R. Comfort, Argonne National Laboratory Report

No. PHY-1970 B (unpublished); we are grateful to Dr. Comfort for making the program available to us.
[23]Written by P. D. Kunz; we are grateful to Dr. Kunz for making the code available to us.
[24]B. Zeidman, J. L. Yntema, and G. R. Satchler, in *Proceedings of the Rutherford Jubilee International Conference*, edited by J. B. Birks (Academic, New York, 1961), p. 515.
[25]W. R. Smith and E. V. Ivash, Phys. Rev. 131, 304 (1963).
[26]W. Fitz, R. Jahr, and R. Santo, Nucl. Phys. A101, 449 (1967).
[27]A. A. Cowley, G. Heymann, R. L. Keizer, and M. J. Scott, Nucl. Phys. 86, 363 (1966).
[28]J. A. R. Griffith, M. Irshad, O. Karban, S. W. Oh, and S. Roman, Nucl. Phys. A167, 87 (1971).
[29]A. J. Frasca, R. W. Finlay, R. D. Koshel, and R. L. Cassola, Phys. Rev. 144, 854 (1966).
[30]Written by F. G. Perey; we are indebted to Dr. Perey for making the code available to us.
[31]See, for example, N. Austern, *Direct Nuclear Reaction Theories* (Wiley-Interscience, New York, 1970).
[32]P. J. A. Buttle and L. J. B. Goldfarb, Proc. Phys. Soc. Lond. 83, 701 (1964).
[33]D. Wilmore and P. E. Hodgson, Nucl. Phys. 55, 673 (1964).
[34]H. F. Lutz, J. B. Mason, and M. D. Karvelis, Nucl. Phys. 47, 521 (1963).
[35]J. Y. Park, J. L. Duggan, P. D. Miller, M. M. Duncan, and R. L. Dangle, Nucl. Phys. A134, 277 (1969).
[36]See, for example, P. E. Hodgson, *The Optical Model of Elastic Scattering* (Oxford U. P., London, 1963).
[37]G. R. Satchler, *Lectures in Theoretical Physics-Nuclear Structure Physics* (Univ. of Colorado Press, Boulder, 1966), p. 73.
[38]H. Fuchs and R. Santo, Phys. Lett. 24B, 234 (1967).
[39]See, for example, J. P. Schiffer, in *Isospin in Nuclear Physics*, edited by D. H. Wilkinson (North-Holland, Amsterdam, 1969), Chap. 13.